

High-frequency properties and magnetic resonance in Nd_2CuO_4

A. I. Smirnov

Institute of Physics Problem, USSR Academy of Sciences

S. N. Barilo and D. I. Zhigunov

Institute of Solid State Physics and Semiconductors, Academy of Sciences, Belorussian SSR

(Submitted 23 July 1991)

Zh. Eksp. Teor. Fiz. **100**, 1690–1698 (November 1991)

Three antiferromagnetic-resonance modes have been observed in single-crystal Nd_2CuO_4 , two excited by a magnetic field and one by an hf electric field. An anomalous temperature dependence of the high-frequency losses, with singularities near the spin-flip temperatures, has been observed.

INTRODUCTION

The magnetic properties and structure of Nd_2CuO_4 are of interest both from the standpoint of superconductivity—this compound was the first used to obtain high-temperature superconductors with electron carriers—and from the standpoint of its magnetic properties—the quasi-two-dimensional antiferromagnetic ordering of the Cu^{2+} in the CuO_2 layers is combined here with the presence of a paramagnetic subsystem of Nd^{3+} ions.

The ordering structure and the magnetic properties of Nd_2CuO_4 ions were already repeatedly investigated.^{1–13} This substance is related to the pioneer La_2CuO_4 of high-temperature superconductivity, but has a different tetragonal crystal-lattice modification and contains also a rare-earth magnetic subsystem made up of the neodymium ions. In contrast to the octahedral surrounding of the copper ions by oxygen ions in La_2CuO_4 , each copper ion in Nd_2CuO_4 is surrounded by only four oxygen ions (see, e.g., Ref. 1). The Nd_2CuO_4 crystal lattice undergoes at 300 K a structural transition in which the tetragonal character of the lattice is preserved, while the unit-cell volume is quadrupled through the displacements of the copper ions along their four sides of the basal square, so that a square along the perimeter can be traced along the displacement directions.²

An antiferromagnetic ordering is produced in Nd_2CuO_4 below $T_N = 250$ K, followed at $T_I = 70$ K by an abrupt rearrangement of the spin structure, a return to the initial spin orientation at 30 K, and one more gradual structure change due to ordering of the neodymium subsystem.^{1,2,3} This ordering is revealed not only by the change of the neutron-diffraction reflections, but also by the smeared peaks of the magnetic susceptibility¹¹ and of the heat capacity.¹² Three types of spin ordering are thus observed, which we shall designate as phases 1, 2, and 3. In phase 3 the spin configuration of the copper ions is the same as in phase 1, but at low temperatures the magnetizations of the neodymium sublattices are appreciable.

The crystal symmetry below the structural-transition temperature permits the presence of six antiferromagnetic structures⁸ with the spins arranged in the basal plane. Neutron-diffraction data in each of phases 1, 2, and 3 can be incontrovertibly interpreted on the basis of two models.

In the first model² the spin structure of phase 1 is assumed to be noncollinear and have four sublattices (structure τ_2 in the notation of Ref. 8). It can be represented as a superposition of two collinear antiferromagnetic structures

with antiferromagnetism vectors perpendicular to one another along the sides of the basal square of the high-temperature crystallographic modification. One antiferromagnetic subsystem is made up of copper ions in the basal planes of the unit cell, and the other by copper ions in positions that center the unit-cell volume. At 70 K the angles between the spins of the antiferromagnetic subsystems change—the 90° angles become -90° and vice versa. This produces phase 2 (structure τ_8 in Ref. 8). A return to phase 1 occurs at 30 K.

In the second model description¹ of the neutron diffraction data the crystal is represented as subdivided into domains of antiferromagnetic phases with spin ordering along the $[110]$ and $[1\bar{1}0]$ axes. A transition from the La_2NiO_4 collinear structure into a collinear La_2CuO_4 structure (the spin orientation changes from parallel to perpendicular to the structure propagation vector) and back is assumed at the reorientation points.

Neither description of the neutron-diffraction data contradicts experiment (see the discussion, Refs. 4 and 5). A strong argument favoring a noncollinear model is the result of Ref. 6, where application of a magnetic field causes a conversion of the aggregate of the neutron-diffraction reflection into a reflection system typical of a single-domain collinear structure. This conversion has no noticeable hysteresis, thus offering evidence in favor of a model that assumes a noncollinear four-sublattice structure rather than domains of collinear phases.

In addition to the analysis of possible antiferromagnetic structures possible in the crystallographic structure of Nd_2CuO_4 , Ref. 8 contains also an analysis of homogeneous spin oscillations in a zero field and predicts the presence in Nd_2CuO_4 of a linear magnetoelectric effect due to exchange interaction.

The magnetization curves of Nd_2CuO_4 were investigated in Ref. 7 at a temperature lower than 2 K. Two types of spin-reorientation transitions with respect to the magnetic field were observed. The first is revealed by a kink on the magnetization curve when the magnetic field is oriented in the $[110]$ direction of the crystal. In the τ_2 structure this direction is inclined 45° to the spins of both antiferromagnetic subsystems. This transition is apparently the end of the rotation of the two antiferromagnetic subsystems perpendicular to the magnetic field. The second transition with a magnetization jump was observed in Ref. 7 when the field was directed along $[100]$, and its nature remains unclear.

We study in the present paper the spin dynamics of anti-

ferromagnetic Nd_2CuO_4 —the high-frequency magnetic losses and the magnetic resonance. A study of the spin-oscillation spectrum can cast light on the type of the structure, since the antiferromagnetic resonance spectrum of a noncollinear four-sublattice structure contains according to Ref. 8 three acoustic modes and one exchange mode, as against one exchange and one acoustic for a collinear one.

EXPERIMENTAL PROCEDURE AND SAMPLES

A free-passage type microwave spectrometer with a rectangular cavity measuring $7.2 \times 3.4 \times 20$ mm was used to measure the high-frequency losses and record the absorption lines in a magnetic field. It has a number of natural frequencies in 30–80 GHz range. A cavity with a sample measuring $1 \times 1 \times 0.7$ mm was placed in a vacuum jacket that permitted regulation of the sample temperature in the range 1.3–300 K. A constant magnetic field up to 60 kOe was produced by a superconducting solenoid.

To measure the temperature dependence of the magnetic losses χ'' we used the TE_{014} oscillation of a cavity having a frequency 36 GHz and a Q of 1000. To decrease the effect of the electric losses ε'' on χ'' the sample was glued-on outside the cavity, covering a hole of 0.8 mm diameter drilled in the cavity wall at the peak of the high-frequency magnetic field. The wall thickness was 0.2 mm. This procedure prevents the onset of a high-frequency electric field in the sample volume without decreasing the sample itself, and preserves its volume to ensure sufficient sensitivity for the study of the magnetic-resonance spectra. The filling factor for such a sample placement was determined by comparing the signals through the sample located inside and outside the cavity near the hole.

The imaginary part of the rf magnetic susceptibility χ'' was determined from the relation

$$\frac{u}{u_0} = \frac{1}{1 + \chi'' \eta Q},$$

where η is the cavity filling factor, and u and u_0 are the signals passing through the cavity in the presence and absence of sample, respectively.

The electric losses were likewise measured by placing the sample outside the cavity, on an opening drilled at the location of the maximum of the hf electric field.

The dependences of the absorption on the magnetic field were obtained mainly with the sample placed inside the cavity at the location of the maximum magnetic field of the TE_{014} , with a polarization perpendicular to the constant field. The sample could be rotated in this location relative to the direction of the external magnetic field.

The objects investigated were Nd_2CuO_4 single crystals grown in a platinum crucible from a melt of ultrapure copper oxide, on a single-crystal seed on a platinum holder, in the presence of an axial temperature gradient. The temperature was lowered at a rate 0.5–1° per day. During the concluding stage of its growth, the seed was rotated slowly at 2–5 rpm.

The grown crystal was a disk 70 mm in diameter and 2 mm thick. The samples used in the investigations were parts of this disk. Control x-ray, neutron-scattering, and neutron-topography experiments performed at the Kurchatov Atomic Energy Institute have shown that the single crystal constituted a single block. The rocking-curve widths did not

exceed 8°. The lattice constants were $a = 3.944$ Å and $c = 12.17$ Å, respectively.

RESULTS OF EXPERIMENT

A. Absorption in a microwave magnetic field

The temperature dependence of the imaginary part of the high-frequency susceptibility χ'' at 36 GHz is shown in Fig. 1. It is nonmonotonic, with the absorption increasing as the temperature is lowered. The absorption begins to increase at $T_N = 250$ K, and abrupt absorption changes are observed in vicinities of the transition temperatures 70 K and 30 K. The ε'' loss in an electric high-frequency field is smaller by about one order than χ'' in the entire temperature range. This rules out a possible contribution to the observed χ'' from losses connected with the sample conductivity.

The dependences of the signal passing through the cavity on the magnetic field at 1.3 K and at 36 and 72 GHz are shown in Figs. 2a and 2b. A family of curves is shown for different values of the angle φ between the magnetic-field direction and the [100] axis. These plots have complicated forms—a curve can have up to three minima (corresponding to absorption maxima), some curves even show breaks and jumps. The fields of the signal minima are labeled H_1 , H_2 , and H_3 , respectively, the break field H_b , and the jump field H_c . The fields H_b and H_c do not depend on the frequency of the signal used to determine them, and agree well to the field values given in Ref. 7 for spin-reorientation transitions. The dependences of the aforementioned characteristic fields obtained at 36 GHz on the angle φ are shown in Fig. 3a, while the dependences of H_b and H_c on φ , obtained at various frequencies, are shown in Fig. 3b.

Families of curves similar to those in Fig. 2 were obtained at various frequencies. All are similar in form to those of Fig. 2a, except that above 42 GHz there is no minimum corresponding the field H_1 . At these frequencies, the transmitted signal increases monotonically when the field changes from 0 to H_b , as in Fig. 2b.

The fields H_1 and H_3 turned out to be frequency dependent and their plots for fields along [100] and [110] are shown in Figs. 4a and 4b. The field H_2 is independent of frequency within the limits of measurement errors.

The temperature variation of the dependence of the absorption on the magnetic field is shown in Figs. 5a and 5b for

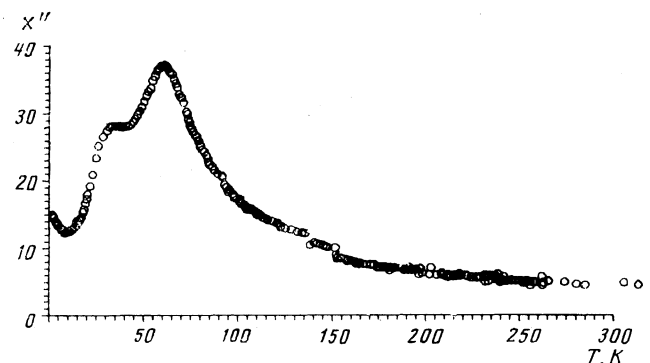


FIG. 1. Imaginary part of high-frequency susceptibility vs temperature at 36 GHz.

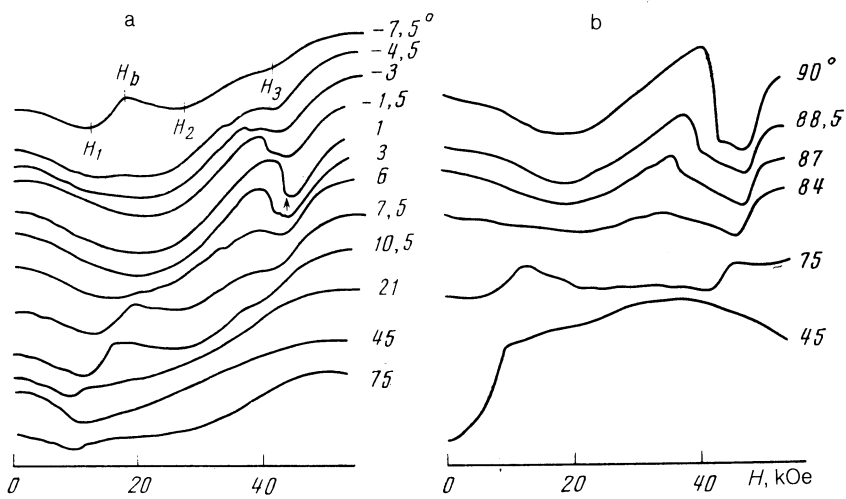


FIG. 2. Signal passing through cavity vs magnetic moment: a) at 36 GHz, b) at 72 GHz. The numbers on the curves denote the angles in the crystal basal plane between the field direction and the [100] axis. $T = 1.3$ K. The arrow at the curve for $\varphi = 1^\circ$ marks the field H_c .

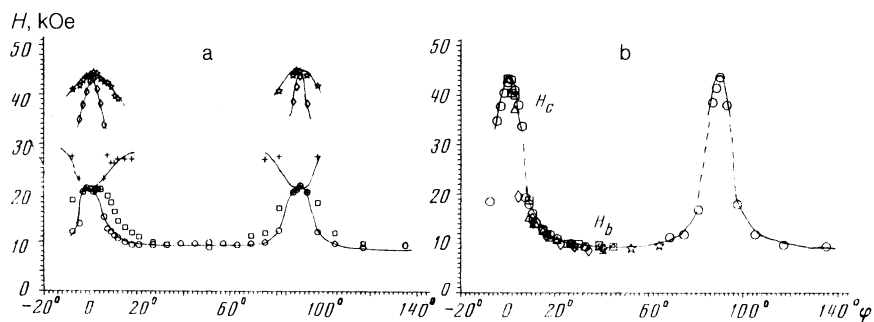


FIG. 3. a—The fields $H_{1,2,3}$ vs the angle between the field and the [100] axis in the crystal basal plane, obtained at 36 GHz; b—fields $H_{b,c}$ vs the field inclination angle in the basal plane, obtained at various frequencies. $T = 1.3$ K.

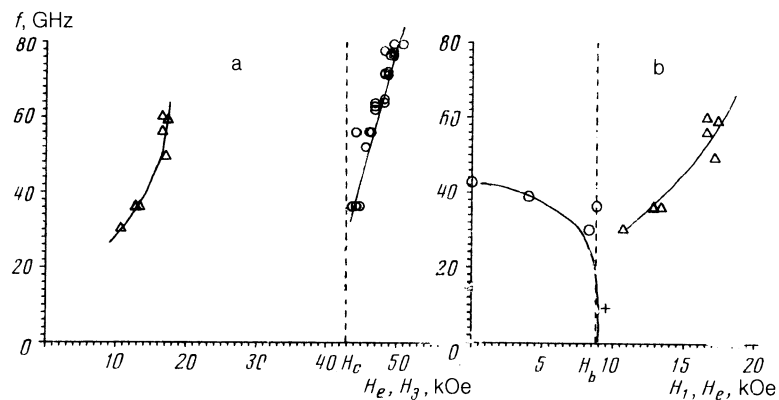


FIG. 4. Resonant absorption spectra: a—for magnetic field oriented along the [100] axis, b—along [110]. $T = 1.3$ K.

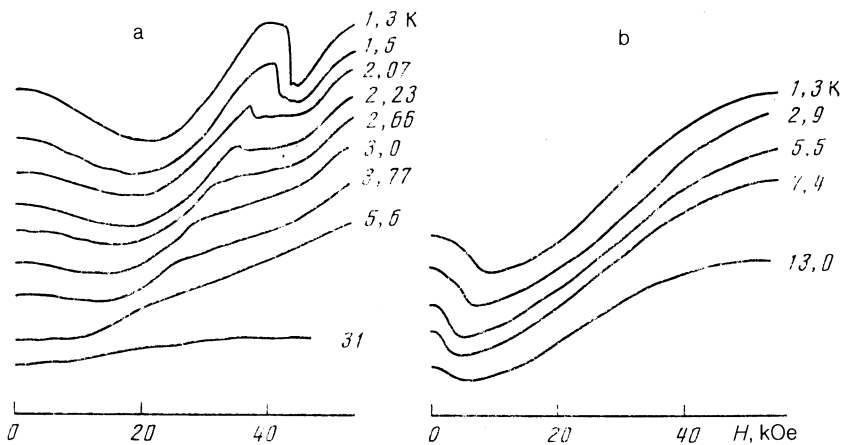


FIG. 5. Signal passing through cavity vs magnetic field, at various temperatures. a— $H \parallel [100]$, b— $H \parallel [110]$.

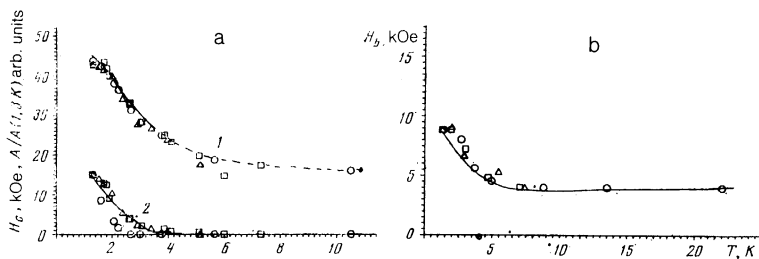


FIG. 6. a—Field H_c and amplitude of absorption discontinuity in this field vs temperature, b—temperature dependence of field H_b .

two field orientations, and is generalized in Figs. 6a and 6b. The resonant-absorption line corresponding to the field H_3 becomes smooth when the temperature is raised above 2 K. The transition in the field H_c also vanishes when the temperature is raised above 10 K. As seen from Fig. 6a, with rise of temperature the absorption discontinuity decreases to zero at $T = 3$ K and changes into a break that is observed up to 10 K. The resonance in the field H_1 and the transition in the field H_b are observed all the way to 30 K. A resonance similar to the absorption in the field H_1 was observed in Ref. 9 at 9 GHz.

In all the dependences of the transmitted signal on the magnetic field one can trace a smooth decrease of the losses with increase of the magnetic field. This is most clearly seen on the plots for $\varphi = 45^\circ$ and on the plots for temperatures higher than 15 K, when the singularities connected with the resonant modes are substantially smoothed out.

B. Absorption in an electric field

The dependence of the transmitted signal on the magnetic field, obtained with the sample placed outside the cavity on an aperture at the peak of the electric field, has the form of a sharp resonance peak and is shown in Fig. 7. The electric-absorption intensity is much lower than the absorption in a high-frequency magnetic field. Therefore when the sample is located inside the cavity in the vicinity of the electric-field maximum one observes the sum of the magnetic and electric absorption signals, making approximately equal contributions, under conditions when the electric field is significantly stronger than the magnetic. The dependence of the frequency of this resonant absorption on the magnetic field is shown in Figs. 4a and 4b. The field H_e of the resonant

absorption of the energy of the electric high-frequency field is independent of the direction of the magnetic field in the basal plane. Electric resonance is observed up to a temperature 50 K.

DISCUSSION OF RESULTS

The results of the preceding section attest to the presence of three resonant-absorption modes in the investigated Nd_2CuO_4 sample—in fields H_1 , H_3 , and H_e . The absorption in field H_2 is apparently nonresonant (no frequency dependence is observed in our frequency range).

The spin dynamics without allowance for the influence of the magnetic field in the Nd_2CuO_4 magnetic structure was considered in Ref. 8. The treatment, based on a symmetry analysis, predicts the presence of four antiferromagnetic-resonance modes, three acoustic and one exchange. Following the authors of this reference, we designate the acoustic modes by a_1 , a_2 , and a_3 , and the exchange mode by e . The frequencies of modes a_1 and a_2 in a zero field are equal. Each of the above modes is excited by definite projections of the magnetic and electric field. The spin oscillations are excited by an electric field as a result of the aforementioned magnetoelectric effect. In the τ_2 structure, the modes a_1 and a_2 presumably realized in Nd_2CuO_4 in the temperature intervals 270–70 and 30–2 K, are excited in particularly a high-frequency field polarized respectively along the [100] and [001] axes, while mode a_3 is excited by an electric field polarized along [001].

It can be assumed in connection with this proposed mode structure of the spin oscillations that the resonance in the field H_1 corresponds to modes a_1 and a_2 , whose frequencies should be degenerate when the field is directed along [110] (equivalently with respect to the two collinear antiferromagnetic subsystems).

We observe no splitting of this mode at field directions that are not exactly aligned with the [110] axis. This may be due either to the small value of this splitting or to the weak field dependences of the frequency of one of the modes, a_1 or a_2 . It can be concluded from our data that the resonant-absorption spectrum corresponding to the field H_1 has a gap between 39 and 42 GHz, for on going from the lower of these frequencies to the higher the plot of the transmitted signal is transformed from one having a minimum into one that increases monotonically.

The resonance absorption line observed in an electric high-frequency field can be presumably identified as a_3 . The polarization of the electric field that excites it agrees with that predicted in Ref. 8.

The resonant absorption produced in the field H_3 at $T < 2$ K is apparently connected with Nd^{3+} ion subsystem

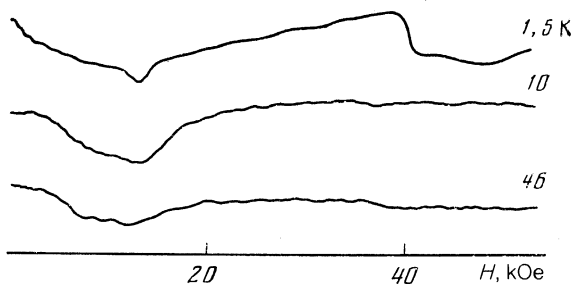


FIG. 7. Transmitted signal vs magnetic field in observation of the electric absorption mode. $\mathbf{H} \parallel [100]$.

which, according to Refs. 2 and 3, becomes ordered at this temperature.

The temperature dependence plotted in Fig. 6a is a phase diagram for a phase transition whose nature is not yet clear. Note that this plot is that of a first-order transition (shows an absorption discontinuity) for temperatures below 3 K and of second order (an absorption break) at higher ones. This line terminates at a critical point near 10 K, where the break smoothens.

The presence of a paramagnetic spin subsystem of Nd^{3+} ions together with an antiferromagnetic matrix of Cu ions is obviously manifested in magnetic-dielectric losses which are anomalous compared with other magnetic dielectrics. A paramagnetic contribution proportional to the reciprocal of the temperature is apparently discernible in the observed temperature dependence of χ'' . A paramagnetic contribution is observed also in the susceptibility χ' (Ref. 11). The substantial influence of the neodymium subsystem on the values of the magnetic high-frequency losses is confirmed by the observable growth of the losses in the course of ordering of the neodymium subsystem close to 2 K. An anomalous behavior near 2 K is observed also for other characteristics measured in a zero field, such as the susceptibility,¹¹ the heat capacity,¹² and the nuclear quadrupole resonance spectrum.¹³

It is possible that the smooth decrease of the losses with increase of the magnetic field is due to the decrease of the losses by suppression of the magnetization fluctuations of the neodymium subsystem by the magnetic field (according to Ref. 7 the magnetic moment saturates in a field close to 60 kOe).

CONCLUSIONS

Three absorption modes were observed, two magnetic and one electric. Two (one magnetic and the electric) are presumably acoustic antiferromagnetic-resonance modes in the noncollinear structure of the ordered Cu spins, and the third corresponds to an ordered subsystem of Nd spins at a temperature below 1.7 K. A gap was determined for one of the modes. A more complete identification of the observed absorption of the energy of the high-frequency magnetic and

electric fields calls for calculation of the antiferromagnetic-resonance spectra with allowance for the magnetic field and of the rare-earth spin subsystem.

A phase diagram, with the magnetic field and temperature as coordinates, was obtained for a phase transition whose nature is not yet clear. This transition is of first order at low temperature and becomes of second order when the temperature is raised.

An anomalous temperature dependence of the magnetic dielectric losses was observed. The losses increase when the temperature is lowered, have singularities near the spin-reorientation temperatures, and increase in the low-temperature region as the neodymium subsystem becomes ordered.

The author thanks I. M. Vitebskiĭ, V. I. Marchenko, and V. L. Sobolev for stimulating discussions.

¹Y. Endoh, M. Matsuda, K. Yamada, K. Kakurai, Y. Hidaka, G. Shirane, and R. Birgenau, *Phys. Rev. B* **40**, 7023 (1989).

²S. Skanthamumar, H. Zhang, T. W. Clinton, W.-H. Li, J. W. Linn, Z. Fisk, S.-W. Cheong, *Physica (Utrecht)* **C 160**, 124 (1989).

³S. Santhakumar, H. Zhang, T. W. Clinton, I. W. Sumarlinn, W.-H. Li, J. W. Linn, Z. Fisk, and S.-W. Cheong, *J. Appl. Phys.* **67**, 4530 (1990).

⁴S. Skanthakumar, J. W. Lynn, *Physica (Utrecht)* **C 170**, 175 (1990).

⁵K. Yamada, K. Kakurai, and Y. Endoh, *ibid.* **C 165**, 131 (1990).

⁶D. Petitgrand, A. H. Moudden, P. Galez., P. Boutrouille, *J. of the Less Common Metals*, **164-165**, 768 (1990).

⁷O. Kondo, M. Ono, T. Yosida, N. Kontani, Y. Chiba, K. Sugiyama, A. Yamagishi, M. Hikita, Y. Hidaka, and M. Date, *J. of Magnetism and Magnetic Materials*, **90-91**, 79 (1990).

⁸V. A. Blinkin, I. M. Vitebskii, O. D. Kolotii, N. M. Lavrinenko, V. P. Seminozhenko, V. L. Sobolev *et al.*, *Zh. Eksp. Teor. Fiz.* **98**, 2098 (1990) [*Sov. Phys. JETP* **71**, 1179 (1990)].

⁹N. Kontani, Y. Chiba, K. Sugiyama, Y. Hidaka, and M. Date, *J. Phys. Soc. Jpn.* **59**, 3019 (1990).

¹⁰V. V. Eremenko, S. A. Zvyagin, V. V. Pishko, V. V. Tsapenko, S. N. Barilo, and D. I. Zhiguonov, *Pis'ma Zh. Eksp. Teor. Fiz.* **52**, 955 (1990) [*JETP Lett.* **52**, 338 (1990)].

¹¹C. L. Seaman, N. Y. Ayoub, T. Bornholm, E. A. Early, S. Ghamaty, B. W. Lee, J. T. Markert, J. J. Neumeier, P. K. Tsai, and M. B. Maple, *Physica C (Utrecht)* **159**, 391 (1989).

¹²S. Ghamaty, B. W. Lee, J. T. Markert, E. A. Early, T. Bornholm, C. L. Seaman, and M. D. Maple, *ibid.* **217** (1989).

¹³Y. Yoshinari, H. Yasuoka, T. Shimizu, H. Takagi, Y. Tokura, and S. Uchida, *J. Phys. Soc. Jpn.* **59**, 36 (1990).

Translated by J. G. Adashko